



UNIVERSITY OF LEEDS

This is a repository copy of *Dynamics of carving runs in alpine skiing. II. Centrifugal pendulum with a retractable leg.*

White Rose Research Online URL for this paper:

<https://eprints.whiterose.ac.uk/158136/>

Version: Accepted Version

Article:

Komissarov, SS orcid.org/0000-0003-4545-9774 (2022) Dynamics of carving runs in alpine skiing. II. Centrifugal pendulum with a retractable leg. *Sport Biomechanics*, 21 (2). pp. 912-939. ISSN 1476-3141

<https://doi.org/10.1080/14763141.2020.1788630>

© 2020 Informa UK Limited, trading as Taylor & Francis Group. This is an author produced version of an article, published in *Sports Biomechanics*. Uploaded in accordance with the publisher's self-archiving policy.

Reuse

Items deposited in White Rose Research Online are protected by copyright, with all rights reserved unless indicated otherwise. They may be downloaded and/or printed for private study, or other acts as permitted by national copyright laws. The publisher or other rights holders may allow further reproduction and re-use of the full text version. This is indicated by the licence information on the White Rose Research Online record for the item.

Takedown

If you consider content in White Rose Research Online to be in breach of UK law, please notify us by emailing eprints@whiterose.ac.uk including the URL of the record and the reason for the withdrawal request.



eprints@whiterose.ac.uk
<https://eprints.whiterose.ac.uk/>

1 Dynamics of carving runs in alpine skiing.
2 II. Centrifugal pendulum with a retractable leg.

3 Serguei S. Komissarov
4 Department of Applied Mathematics
5 The University of Leeds
6 Leeds, LS2 9JT, UK
7 e-mail: s.s.komissarov@leeds.ac.uk

8 Abstract

In this paper we present an advanced model of centrifugal pendulum where its length is allowed to vary during swinging. This modification accounts for flexion and extension of skier's legs when turning. We focus entirely on the case where the pendulum leg shortens near the vertical position, which corresponds to the most popular technique for the transition between carving turns in ski racing, and study the effect of this action on the kinematics and dynamics of these turns. In particular, we find that leg flexion on approach to the summit point is a very efficient way of preserving the contact between skis and snow. The up and down motion of the skier centre of mass can also have strong effect of the peak ground reaction force experienced by skiers, particularly at high inclination angles. Minimisation of this motion allows a noticeable reduction of this force and hence of the risk of injury. We make a detailed comparison between the model and the results of a field study of slalom turns and find a very good agreement. This suggests that the pendulum model is a useful mathematical tool for analysing the dynamics of skiing.

9
Keywords: alpine skiing, modelling, balance/stability, performance

10 **Introduction**

11 The skiing of expert skiers is characterised by smooth and rhythmic moves which
12 are very reminiscent of a pendulum or metronome. This analogy invites mathematical
13 modelling of skiing based on the pendulum action, which can be traced back to the
14 pioneering work by Morawski (1973). They argued that a skier can be treated as
15 pendulum's load and their skis as its pivot point. Such an inverted pendulum, with

16 its load located above its pivot, can be prevented from falling under the action of the
 17 gravity force, provided the pivot is allowed to slide horizontally under the action of a
 18 control force which pushes it in the direction to which the pendulum is leaning.

19 Recently we proposed a variant of this model, where the control force is replaced
 20 with the snow reaction force naturally emerging in carving turns (Komissarov, 2020).
 21 In perfect carving turns, the snow reaction force makes skis to move along quasi-
 22 circular arcs whose centre is located on the same side of the arc as the skier centre
 23 of mass (CM). Thus the skis are forced to return back under the CM, like in the
 24 controlled inverted pendulum. On hard snow, the local curvature radius of carved ski
 25 tracks is fully determined by the ski sidecut radius R_{sc} (which is a fixed parameter of
 26 the skis) and the local ski tilt (or inclination) angle to the slope Ψ (Howe, 1983, page
 27 101). Hence given the skis speed, we can immediately find their acceleration.

28 The dynamics of such pendulum is easy to analyse in the accelerated frame
 29 of its pivot (skis), where the load is subjected to the gravity force, the leg reaction
 30 force, and the centrifugal force determined by the pendulum inclination. The gravity
 31 pushes the load towards the ground, the centrifugal force pushes it back to the vertical
 32 position and the leg reaction force controls the separation between the load and the
 33 pivot. We called such a pendulum centrifugal (Komissarov, 2020).

34 In addition to the vertical equilibrium of the traditional inverted pendulum, the
 35 centrifugal pendulum can have two more equilibria, one on each side, where the total
 36 torque due to the gravity and centrifugal force vanishes. These balanced (equilibrium)
 37 positions of the pendulum are inclined to the vertical by the angle

$$\Psi_{eq} = \arcsin \zeta, \quad (1)$$

38 where

$$\zeta = \frac{V^2}{gR_{sc}} \quad (2)$$

39 and V is the ski speed. Since skiing practitioners often describe balanced body posi-
 40 tion as an essential ingredient of advanced skiing, it may seem only natural to focus
 41 on the incline equilibria and the properties of corresponding carving turns. Theoret-
 42 ical analysis of such quasi-static turns has been carried out in several studies (e.g.
 43 Howe, 1983; Jentschura & Fahrbach, 2004; Komissarov, 2018). However, the inclined
 44 equilibria exist only when $\zeta < 1$ (the subcritical regime). This condition is equivalent
 45 to the upper limit $V < \sqrt{gR_{sc}}$ on the skier speed. Although this limit is quite high,
 46 the typical speeds of top ski racers are still higher (Komissarov, 2018, 2020), show-
 47 ing that skiing in balance is not the only option. Moreover, the inclined equilibria
 48 are unstable and hence impossible to sustain, unless an additional control force is
 49 introduced into the system (Komissarov, 2018, 2020).

50 Fortunately, it turns out that the model of centrifugal pendulum also allows
 51 oscillations about the vertical equilibrium (Komissarov, 2020). In the subcritical
 52 regime their amplitude is limited from above by Ψ_{eq} . In the supercritical regime
 53 ($\zeta > 1$) the amplitude is not limited, apart from the obvious limit $\Psi < 90^\circ$ set by the

54 presence of solid ground. In these solutions the pendulum is never in equilibrium, and
 55 the forces are never balanced. This finding shows that the force balance is actually
 56 not an inherent feature of ski turns and invites us to reexamine the way we see alpine
 57 skiing. In Komissarov (2020), we associated the oscillatory solutions with the dynamic
 58 rhythmic turns performed by expert skiers and racers.

59 So far, we have explored only the highly simplified case where the length of the
 60 pendulum leg remains unchanged. As a result, the trajectory of its load is a circular
 61 arc symmetric about the vertical direction and hence near the vertical position the
 62 load experiences a downward acceleration. In the subcritical regime, this acceleration
 63 can be provided solely by the gravitational force. In the supercritical regime, the leg
 64 tension is also required when the oscillation amplitude exceeds a certain limit. In this
 65 case the pivot is pulled away from the ground. Since skis are not affixed to the snow,
 66 they are expected to lift off it in this regime. In fact, in skiing there are occasions
 67 when both skis are indeed lifted off the snow. Sometimes this is made intentionally,
 68 e.g. during execution of the so-called “dolphin turn”, but more often accidentally,
 69 e.g. when skiing over a bump. In ski racing this is generally undesirable due to
 70 the inevitable loss of the turning action. Skiers have learned to negate this effect
 71 by flexing their legs when going over a real bump or the so-called “virtual bump” in
 72 the transition between turns (e.g. LeMaster, 2010, page 40). Hence we hypothesise
 73 that by allowing the pendulum leg to vary in length during its swing we may be able
 74 to avoid it being pulled away from the ground at the summit point in the regimes
 75 consistent with the practice of alpine racing. The development and investigation of
 76 such an advanced model is the main aim of the study described in this paper.

77 Methods

78 The basic features of the model are presented in the first paper of the series
 79 (Komissarov, 2020). Therefore here we only briefly describe the common basics and
 80 focus on the new developments. A load of mass m is affixed to the upper end of
 81 a massless rod of length l whose lower end is attached to a stationary pivot point
 82 on a flat horizontal surface. To describe the pendulum motion quantitatively, we use
 83 Cartesian coordinates with the origin at the pivot point and the basis vectors \mathbf{i} , \mathbf{j} and
 84 \mathbf{k} such that the pendulum moves in the plane orthogonal to \mathbf{i} , and \mathbf{k} points upwards
 85 in the vertical direction. The position vector \mathbf{r} connects the origin with the affixed
 86 mass. The inclination angle Ψ is the angle between the vertical direction and the
 87 pendulum. We agree that it is positive in the clockwise direction and negative in the
 88 anti-clockwise direction.

89 The load is subject to the vertical gravity force

$$\mathbf{F}_g = -mg\mathbf{k}. \quad (3)$$

90 the centrifugal force

$$\mathbf{F}_c = -(mV^2/R)\text{sgn}(\Psi)\mathbf{j}, \quad (4)$$

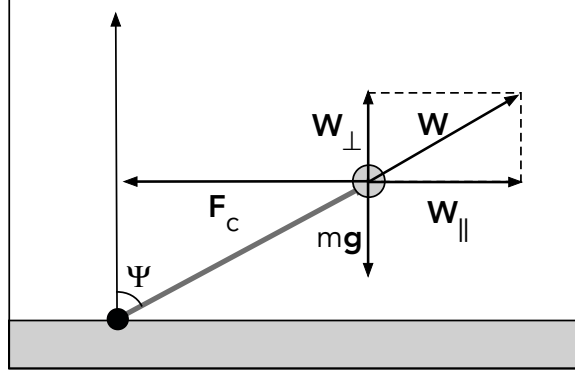


Figure 1. The diagram of forces acting on the pendulum load. F_c is the centrifugal force, mg is the gravity force, and W is the reaction force of the pendulum leg.

where V is the ski speed, R is the curvature radius of the ski trajectory and

$$\text{sgn } \Psi = \begin{cases} +1 & \text{if } \Psi > 0; \\ 0 & \text{if } \Psi = 0; \\ -1 & \text{if } \Psi < 0. \end{cases}$$

91 is the sign function, and the reaction force of the leg W , which ultimately determines
92 the distance between the load and the pivot point, the leg length.

93 For a perfect carving turn on hard snow

$$R = R_{sc} \cos \Psi \quad (5)$$

94 (Howe, 1983; Lind & Sanders, 1996). Strictly speaking, this relation is based on the
95 assumption that the penetration of the snow surface by the skis is negligibly small.
96 The values measured by Reid, Haugen, Gilgien, Kipp, and Smith (2020) in a field
97 study of slalom turns performed by elite racers on hard snow are in agreement with
98 equation (5) up to $\Psi = 70^\circ$.

99 The radial motion of the pendulum mass m is described by the equation

$$ma_r = W + F_{c,r} + F_{g,r}, \quad (6)$$

100 where

$$a_r = \frac{d^2 l}{dt^2} - l \left(\frac{d\Psi}{dt} \right)^2 \quad (7)$$

101 is its radial acceleration and W is the reaction force of the pendulum leg. In the
102 model we ignore leg's mass, which implies that $W = F_{GR}$, the ground reaction force
103 at the pivot point. When $W < 0$, this is a tension force which resists the action
104 aimed at extending the leg. When $W > 0$, this is a compression force which resists

105 the action aimed at shortening the leg. In the latter case, W is the effective weight of
 106 the load. When measured in the units of mg , the effective weight is called a g-force.
 107 In skiing it corresponds to the ground reaction force originated at the skis (Gilgien,
 108 Spörri, Kröll, Crivelli, & Müller, 2014).

109 The swinging motion of the pendulum is governed by the equation

$$\frac{d\mathbf{M}}{dt} = \mathbf{K}, \quad (8)$$

110 where $\mathbf{M} = m\mathbf{r} \times \mathbf{u}$ is the pendulum angular momentum, $\mathbf{K} = \mathbf{r} \times \mathbf{F}_g + \mathbf{r} \times \mathbf{F}_c$ is the total
 111 torque about the pivot point, and $\mathbf{r} = l \sin \Psi \mathbf{j} + l \cos \Psi \mathbf{k}$ is the position vector (Landau
 112 & Lifshitz, 1969). The velocity vector \mathbf{u} can be split into the components parallel and
 113 perpendicular to the position vector, $\mathbf{u} = \mathbf{u}_{\parallel} + \mathbf{u}_{\perp}$, where $\mathbf{u}_{\perp} = l(d\Psi/dt)(\cos \Psi \mathbf{j} -$
 114 $\sin \Psi \mathbf{k})$. Upon the substitution of all these expressions, equation (8) reduces to

$$\frac{d}{dt} \left(l^2 \frac{d\Psi}{dt} \right) = gl \sin \Psi - l \frac{V^2}{R_{sc}} \operatorname{sgn} \Psi. \quad (9)$$

115 Since the leg reaction force \mathbf{W} is aligned with \mathbf{r} , it makes zero contribution
 116 to the torque \mathbf{K} and effects the swinging motion only via the leg length. Instead of
 117 prescribing this force and then solving for the leg length, we may simply prescribe the
 118 leg length and then proceed with solving equation (9). The corresponding leg reaction
 119 force can be calculated later, via post-processing of the solution, when needed. This
 120 is exactly how it is done in the basic model, which assumes $l = \text{const}$.

121 Here we assume that the pendulum length is a function of the inclination angle
 122 and write

$$l(\Psi) = l_0 f(\Psi), \quad (10)$$

123 where l_0 is its characteristic length scale and $f(\Psi)$ is a differentiable function, which
 124 we will refer to as the “retraction function”. With this law the pendulum is a closed
 125 system and satisfies the energy conservation law (see Appendix A). In what follows,
 126 we interpret l_0 as the height of skier’s CM from the ground at maximally extended
 127 upright position. For the average adult male height of 180 cm (e.g. Roser, Appel, &
 128 Ritchie, 2020), and the average ratio between the CM height and the total height of
 129 56% (e.g Davidovits, 2018, page 3), l_0 is about one meter. Expert skiers flex their legs
 130 in the transition between turns and extend them during the turn (e.g. Harb, 2006;
 131 LeMaster, 2010; Reid, 2010). This technique corresponds to $f(0) < 1$.

132 We further assume that $f(\Psi)$ is a symmetric function, and hence $f(\Psi) = f(-\Psi)$
 133 and $f'(0) = 0$. In application to skiing, this implies that before and after the transition
 134 between two turns the extension of skier’s legs and the ski tilt angle are related in
 135 exactly the same way. Although there is no reason why this should be the case in real
 136 skiing, the data provided in Reid (2010) shows that this assumption is reasonable.
 137 The degree to which skiers extend and flex their legs also varies from turn to turn,
 138 as dictated by the terrain and individual preferences. Here we ignore this caveat and
 139 focus on the basic effects of the leg action instead.

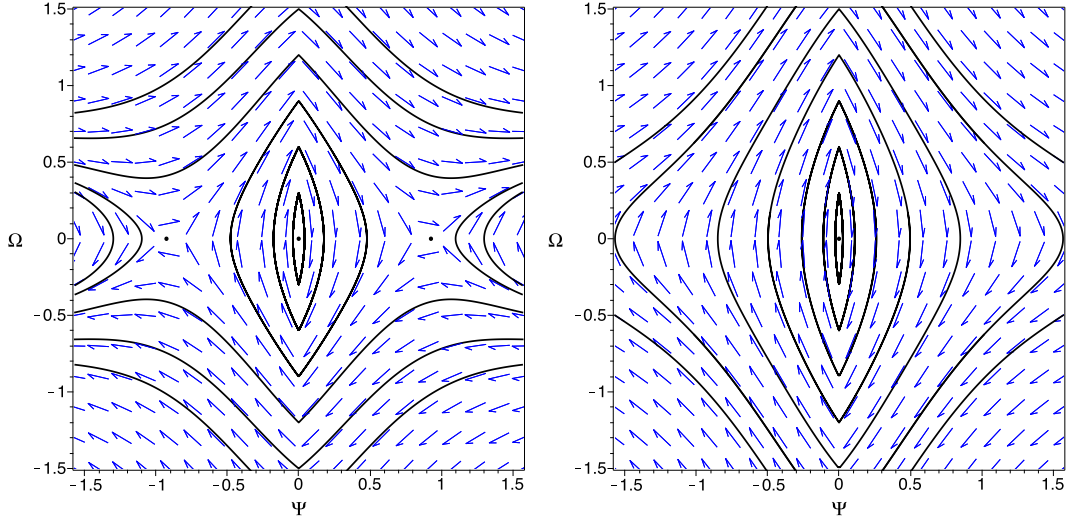


Figure 2. Typical phase portrait of the centrifugal pendulum with a retractable length. The plots correspond to the retraction function of the model B (see section Results for details) with the parameters $b = 0.65$ and $\zeta = 0.8$ (left) and $\zeta = 1.2$ (right). The inclination angle is given in radians.

140 Via introducing the dimensionless time $\tau = t/T$, where $T = \sqrt{l_0/g}$ is the natural
 141 time-scale of the pendulum, equation (9) is reduced to its basic form

$$f(\Psi)\ddot{\Psi} + 2f'(\Psi)\dot{\Psi}^2 = \sin \Psi - \zeta \operatorname{sgn} \Psi, \quad (11)$$

142 where ζ is the speed parameter given by equation (2), and we use the notations $\dot{A} =$
 143 $dA/d\tau$ and $A' = dA/d\Psi$. The first term on the right side of the equation represents
 144 the torque due to gravity, and the second one the torque due to the centrifugal force.
 145 The types of solutions allowed by this equation depend on the value of ζ .

146 To elucidate the properties of a dynamical system described by a second order
 147 ordinary differential equation, it is helpful to convert it into a system of two first
 148 order equations. In our case, the standard conversion yields

$$\begin{aligned} \frac{d\Omega}{d\tau} &= -\frac{2f'(\Psi)}{f(\Psi)}\Omega^2 + \frac{1}{f(\Psi)}(\sin \Psi - \zeta \operatorname{sgn} \Psi) \\ \frac{d\Psi}{d\tau} &= \Omega, \end{aligned} \quad (12)$$

where Ω is the angular velocity of the pendulum. This system allows static solutions (or equilibrium points) which satisfy the condition

$$\frac{d\Omega}{d\tau} = \frac{d\Psi}{d\tau} = 0.$$

149 One of them, $(\Omega, \Psi) = (0, 0)$, describes the vertical position of the pendulum and
 150 corresponds to the skier gliding down the fall line. When $\zeta > 1$ (the supercritical

151 regime) this is the only static solution allowed by the system. When $\zeta < 1$ (the
 152 subcritical regime) there are two more static solutions, $(\Omega, \Psi) = (0, \pm \arcsin(\zeta))$,
 153 which describe inclined positions on both sides of the vertical and correspond to
 154 turns made in perfect balance. Interestingly, these static solutions do not depend on
 155 the form of the retraction function $f(\Psi)$. They are exactly the same as in the case of
 156 the pendulum with fixed leg length. Hence phase portraits corresponding to different
 157 retraction functions are qualitatively the same if we use the same value of ζ . Figure
 158 2 illustrates the properties of these phase portraits using the retraction function B,
 159 described later in Results, as an example. The closed orbits around the origin in the
 160 portrait describe pendulum's oscillations about its vertical position – they correspond
 161 to the dynamic type of carved turns.

162 When simulating the trajectories of ski runs based on the pendulum model it
 163 is convenient to introduce the length scale $\mathcal{L} = R_{sc}$ and the time scale $\mathcal{T} = R_{sc}/V$.
 164 This leads to the dimensionless equations

$$f(\Psi) \frac{d^2\Psi}{ds^2} + 2f'(\Psi) \left(\frac{d\Psi}{ds} \right)^2 = \delta(\zeta^{-1} \sin \Psi - \operatorname{sgn} \Psi), \quad (13)$$

165

$$\frac{d\gamma}{ds} = \operatorname{sgn} \Psi \sec \Psi, \quad (14)$$

166

$$\frac{d\bar{x}}{ds} = \cos \gamma, \quad (15)$$

167

$$\frac{d\bar{y}}{ds} = \sin \gamma, \quad (16)$$

168 where $s = t/\mathcal{T} = Vt/R_{sc}$, $\bar{x} = x/R_{sc}$, $\bar{y} = y/R_{sc}$, γ is the instantaneous angle of
 169 traverse, and the dimensionless parameter $\delta = R_{sc}/l_0$ (Komissarov, 2020). Note that
 170 the independent variable s is actually the distance along the trajectory measured in
 171 the units of sidecut radius. For simplicity, we will use the initial conditions $\bar{x}(0) = 0$,
 172 $\bar{y}(0) = 0$, $\gamma(0) = 0$, $d\Psi/ds(0) = 0$ and $\Psi(0) = \Psi_{max}$. No matter what the dimensional
 173 parameters of the problem are, the dimensionless trajectory $\bar{y} = f(\bar{x})$ is completely
 174 determined by the initial conditions and the dimensionless parameters ζ and δ .

175

Results

176 In the limit of small amplitude ($\Psi \ll \min 1, \zeta$), equation (11) reduces to

$$f(0)\ddot{\Psi} = -\zeta \operatorname{sgn} \Psi. \quad (17)$$

177 This equation has periodic solutions, whose period P depends on their amplitude
 178 Ψ_{max} . When $f(0) = 1$ we recover the basic model with non-retractable leg (Komis-
 179 sarov, 2020). Since upon the substitution $\tau = \sqrt{f(0)}\tilde{\tau}$ equation (17) reduces to its

180 non-retractable form, the period of the retractable solution differs from the period of
 181 the non-retractable solution of the same amplitude only by the factor $f^{1/2}(0)$, namely

$$P = 4f^{1/2}(0) \left(\frac{2\Psi_{max}}{\zeta} \right)^{1/2}. \quad (18)$$

182 Since leg flexion in transition between turns corresponds to $f(0) < 1$, this equation
 183 allows us to conclude that such turn technique yields turns that are shorter in duration
 184 and, given the same speed, in length compared to the case without flexion.

185 While the dimensionless period of pendulum oscillations depends only on ζ and
 186 Ψ_{max} , the dimensional period also scales like $\sqrt{l_0}$, simply because the employed time
 187 scale $T = \sqrt{l_0/g}$. Hence for the same speed, sidecut radius of skis, and the amplitude
 188 of skier's inclination, a shorter skier (with a lower CM) will be making shorter turns
 189 compared to a taller skier (with a higher CM). A little bit more information on the
 190 scaling with l_0 can be extracted from equations (13)-(16). First, equation (13) shows
 191 that $\Psi(s, \delta, \zeta) = F(\delta^{1/2}s, \zeta)$ and hence $s(\Psi, \delta, \zeta) = \delta^{-1/2}S(\Psi, \zeta)$, confirming that the
 192 turn length scales like $\sqrt{l_0}$. (Here $F(x, y)$ and $S(x, y)$ are not some specific functions;
 193 they are introduced simply to expose the dependence of Ψ and s on δ .) Given this
 194 result, equation (14) implies that $\gamma(\Psi, \delta, \zeta) = \delta^{-1/2}\Gamma(\Psi, \zeta)$ and hence

$$\frac{d\bar{x}}{ds} = \cos(\delta^{-1/2}\Gamma(\Psi, \zeta)), \quad (19)$$

195

$$\frac{d\bar{y}}{ds} = \sin(\delta^{-1/2}\Gamma(\Psi, \zeta)). \quad (20)$$

196 From this it follows that as l_0 decreases (and hence δ increases), $d\bar{x}/ds$ increases and
 197 $d\bar{y}/ds$ decreases and hence the trajectory straightens up even if the range of Ψ and
 198 hence the range of the curvature radius R remain the same. Thus, all other things
 199 being equal, shorter skiers make not only shorter but also shallower turns.

200 How skiers flex and extend their legs depends on many factors, including their
 201 level and individual preferences. Here we are not aiming at comprehensive analysis
 202 and rigorous derivation of general conclusions. Instead we focus on the most common
 203 type of the transition between turns in modern ski racing, which involves legs flexion
 204 in transition between turns, and consider in details only two specific examples of the
 205 retraction function. These are illustrated in figure 3

206 Case A

207 We start with the retraction function

$$f(\Psi) = \frac{a}{\cos \Psi}, \quad (21)$$

208 which ensures that maximum retraction occurs in the vertical position ($\Psi = 0$), which
 209 is the transition point between turns (see the left panel of figure 3). Moreover, in this

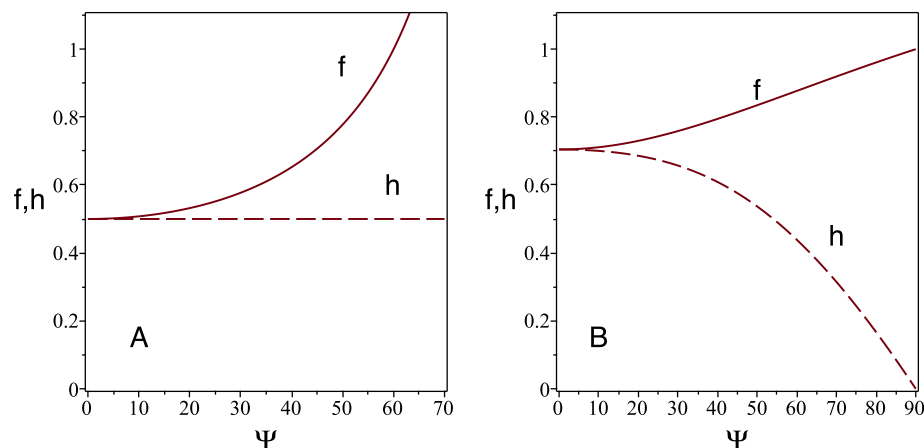


Figure 3. The leg retraction function $f(\Psi)$ and the corresponding height $h(\Psi) = f(\Psi) \cos(\Psi)$ of the pendulum load above the ground in the reference models A (left panel) and B (right panel).

210 model the height of the CM above the ground, $H = l_0 f(\Psi) \cos \Psi$, is constant, and
 211 hence the vertical acceleration of the CM vanishes completely. Thus the snow contact
 212 is preserved at all time. An excellent video demonstrating this leg action was made
 213 available on YouTube by Alltracks Academy (Hetherington, 2016).

214 Since the full leg extension corresponds to $f = 1$, equation (21) implies the
 215 upper limit $\Psi_{lim} = \arccos(a)$ on the inclination angle. Thus, the smaller the value of
 216 a is the larger inclinations angles can be accommodated. However, in the transition
 217 between turns skiers rarely flex their legs beyond the point where the femur bone is
 218 parallel to the slope. This is easy to understand as squatting seriously compromises
 219 human body's manoeuvrability. When the femur bone is parallel to the slope one may
 220 expect a reduction of the CM height by up to a factor of two compared to that in
 221 the fully extended upright position, and hence $a = 0.5$. The corresponding maximum
 222 inclination angle $\Psi_{lim} \approx 60^\circ$. We are not aware of any study set to determine the
 223 lowest position of the CM achievable in the transition between turns of alpine skiing.
 224 However, our expectation agrees with the actual measurements taken in the studies
 225 of the jump biomechanics (Domire & Challis, 2007). In the rest of the paper, we
 226 consider only the case with $a = 0.5$ and refer to it as the model A.

227 Figure 4 compares the trajectory obtained in model A with the trajectory in
 228 the case of fixed leg ($l = l_0$) for the same inclination amplitude. One can see that
 229 in the model A the trajectory has a similar curvature but its turns are shorter. The
 230 reduction of the turn length is consistent with the reduction of the turn period by
 231 the factor $\sqrt{2}$ according to the small amplitude result (18).

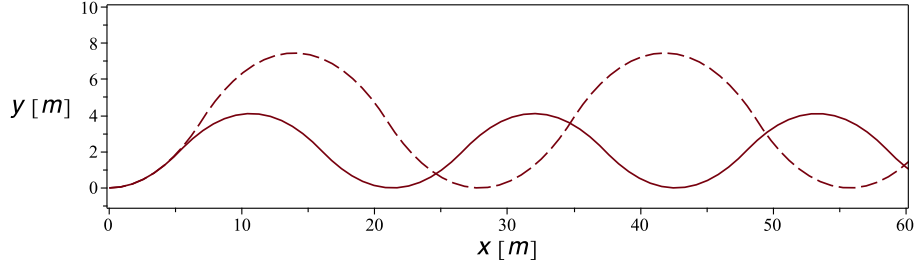


Figure 4. Trajectories of carving runs executed with leg flexion as described in the model A (solid line) and without leg flexion (dashed line; model B with $b = 0$). In both cases $l_0 = 1$ m, $R_{sc} = 14$ m, $V = 13.7$ m/s ($\zeta = 1.37$) and $\Psi_{max} = 60^\circ$.

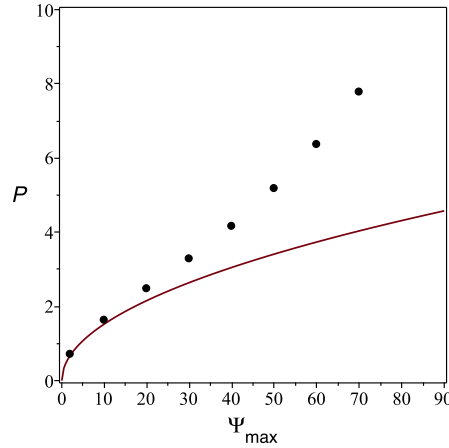


Figure 5. Dimensionless period of the pendulum in the model A with $\zeta = 1.2$. The line shows the period of the small amplitude solution given by equation (22). The dots show the periods of solutions, which were found via numerical integration of equation (11).

232 **Period-amplitude relation.** Since in this model $f(0) = 1/2$, the small-
233 amplitude result (18) reads

$$P = 4 \left(\frac{\Psi_{max}}{\zeta} \right)^{1/2}. \quad (22)$$

234 In the nonlinear regime, the period keeps growing with the amplitude and does this
235 even faster, as this can be seen in figure 5. As a result of this dependence, carving
236 turns with smaller inclination are shorter (see figure 6). They are also straighter
237 because according to Howe's formula smaller Ψ implies smaller curvature of turn's
238 arc. This is similar to what was found in the model with fixed leg length (Komissarov,
239 2020).

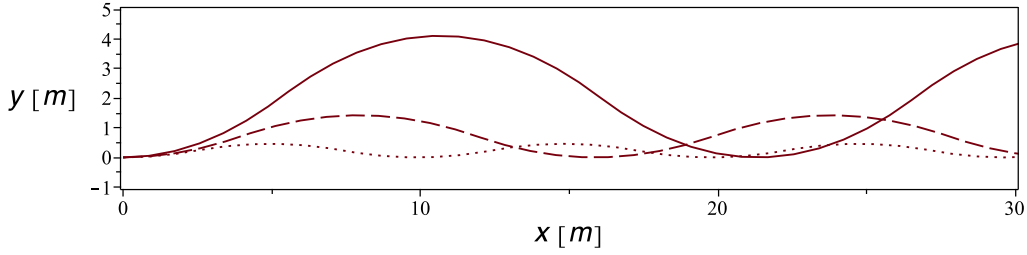


Figure 6. Trajectories of carving run in the model A with for $\Psi_{max} = 60^\circ$ (solid line), $\Psi_{max} = 40^\circ$ (dashed line) and $\Psi_{max} = 20^\circ$ (dotted line). The other parameters are $l_0 = 1$ m, $R_{sc} = 14$ m and $V = 13.7$ m/s ($\zeta = 1.37$).

240 **Ground reaction force.** In the model A, the leg reaction force is always a
 241 compression and the corresponding ground reaction force is

$$F_{GR} = \frac{1}{\cos \Psi}. \quad (23)$$

242 (see Appendix B). Thus, the effective skier's weight does not depend on their speed,
 243 contrary to what one would expect given the fact that the centrifugal force, which con-
 244 tributes to the total loading, is speed-dependent. Instead, it is completely determined
 245 by the skier inclination.

246 For the vertical position ($\Psi = 0$), equation (23) yields $F_{GR} = 1$, which is the
 247 normal weight of the load. This implies that at transition between carving turns the
 248 skis are still loaded quite heavily, making their pivoting problematic. However, in the
 249 case of pure carving, skis are simply rolled from edge to edge without pivoting.

250 At first glance, the lack of dependence of F_{GR} on the speed is a paradox. Indeed,
 251 at low speeds the centrifugal force is small and hence F_{GR} must be close to unity,
 252 which is not supported by equation (23). However, at low speeds the amplitude of
 253 periodic solutions must stay below $\Psi_{eq} = \arcsin(\zeta)$. Because $\Psi_{eq} \rightarrow 0$ as $\zeta \rightarrow 0$, at
 254 low speeds Ψ must be low and hence F_{GR} must be close to unity, as expected. In
 255 contrast, for $\zeta > 1$ the inclination angle can have any value between $-\pi/2$ and $\pi/2$,
 256 and this indirect dependence of F_{GR} on ζ disappears.

257 **Speed dependence of trajectory.** The fact that neither the snow contact
 258 condition nor the ground reaction force constrain the skier speed in this model invites
 259 us to consider the high ζ regime in some detail. In particular, one may wonder how the
 260 skier speed affects the trajectory of their run. Figure 7 shows the results of simulations
 261 for slalom skis with $R_{sc} = 14$ m and the speed parameter varying from $\zeta = 1$ to $\zeta = 10$.
 262 The inclination amplitude of all these runs is the same, $\Psi_{max} = 60^\circ$. One can see that
 263 as ζ increases the turns become shorter and shallower. This could be expected given
 264 the form of the right-hand side of equation (13), which increases with ζ , leading to
 265 faster variation of the inclination angle with the distance along the trajectory. Figure

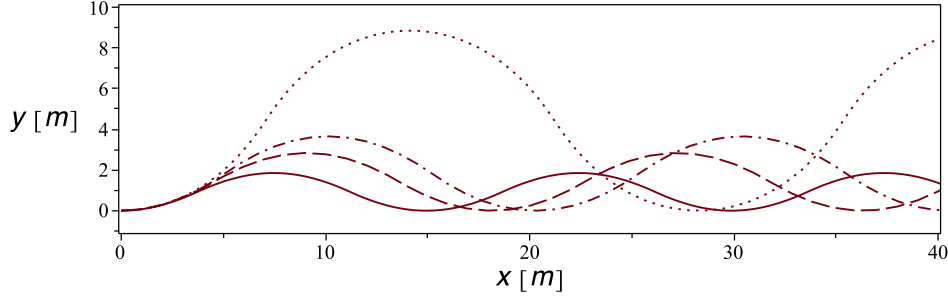


Figure 7. Trajectories in the model A for $\zeta = 1$ (dot line), $\zeta = 1.5$ (dot-dash line), $\zeta = 2$ (dash line) and $\zeta = 10$ (solid line). The other parameters $R_{sc} = 14$ m, $l_0 = 1$ m and $\Psi_{max} = 60^\circ$ are the same for all solutions.

266 7 also suggests that the dependence on ζ weakens as it increases. This is consistent
 267 with the fact that as $\zeta \rightarrow \infty$ the first term on the right-hand side of equation (13)
 268 becomes much smaller compared to the second term and hence the dependence on ζ
 269 vanishes. Hence we should expect the trajectory to approach some asymptotic form.
 270 Figure 6 shows that for $\zeta = 10$ the amplitude of the oscillations along the y axis is
 271 only just above $l_0 \sin \Psi_{max}$, the horizontal amplitude of the pendulum oscillations in
 272 this model. This suggests that the asymptote describes the limiting regime where the
 273 skier CM moves straight down the fall line, unaffected by the side-to-side motion of
 274 the skis underneath it. However, this has not yet been analytically proved.

275 Case B

276 In the case B, we put

$$f(\Psi) = (1 - b \cos \Psi)^{1/3}, \quad (24)$$

277 where b is a parameter. This function has a number of attractive features and this
 278 is why it was chosen. Firstly, for the retractability parameter $b = 0$ we recover
 279 the pendulum of fixed length. Secondly, it allows a relatively simple expression for
 280 the potential energy of the pendulum (see Appendix A). Finally, according to the
 281 measurements made by Reid (2010), during a typical SL turn the height of skier CM
 282 reduces from $h \approx 0.7$ m at the transition down to $h \approx 0.4$ m when the ski inclination
 283 angle reaches $\Psi_{max} \approx 67^\circ$. The right panel of figure 3 shows the leg retraction function
 284 $f(\Psi)$ and the CM-height function $h(\Psi) = f(\Psi) \cos \Psi$ for $b = 0.65$. In this case the
 285 CM height h reduces from 0.70 at $\Psi = 0$ to 0.37 at $\Psi = 67^\circ$. Thus this model
 286 introduces the variability of the CM height which is only a little bit more extreme
 287 than that measured by Reid (2010). In what follows, we use to the case with $b = 0.65$
 288 as a reference model.

289 **Snow contact condition.** Figure 8 compares the ground reaction forces cal-
 290 culated using equation (41) of Appendix B for the case with fixed leg ($b = 0$) and for

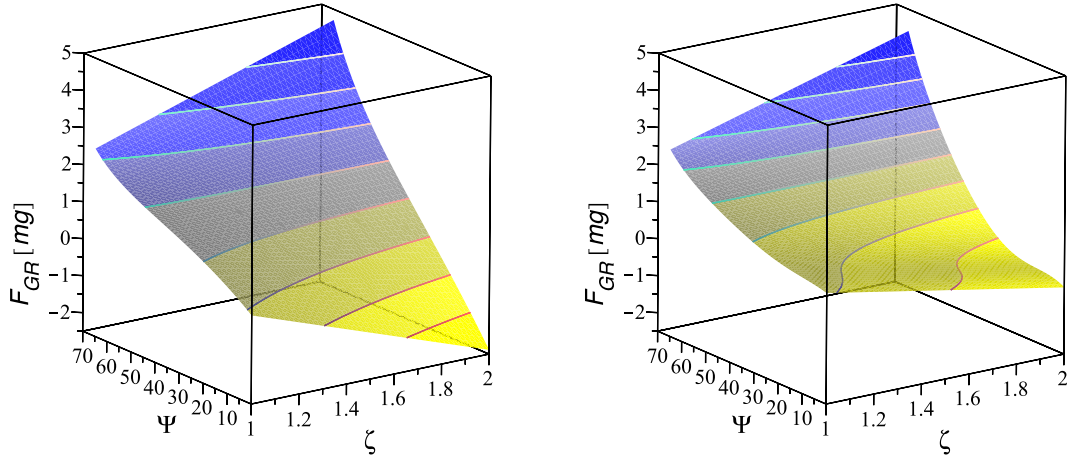


Figure 8. Ground reaction force as a function of ζ and Ψ in the model B with $\Psi_{max} = 65^\circ$. The left panel shows the force in the case of fixed leg ($b = 0$). The right panel shows the force in the case of retractable leg ($b = 0.65$). The force is given in the units of mg .

291 the case with a retractable leg ($b = 0.65$). In both cases the amplitude of pendulum
 292 oscillation $\Psi_{max} = 65^\circ$. Then the force is positive, it is a reaction to the pivot point
 293 is pushed into the ground. When it is negative, it is a reaction to the pivot point
 294 being pulled away from the ground. Skis can play the role of a pivot only when they
 295 are pushed into the snow and we expect them to lift off the snow when the pendulum
 296 model predicts $F_{GR} < 0$.

297 The left panel of figure 8 shows that in the case of fixed leg, $F_{GR} < 0$ near the
 298 vertical position ($\Psi = 0$) for nearly all $\zeta > 1$ and becomes very large near $\zeta = 2$.
 299 In carving turns describes by such solutions, a skier would be catapulted into the air
 300 (cf. Komissarov, 2020). However in the retractable case, the value of F_{GR} near the
 301 vertical position is notably higher, and is actually positive for $\zeta < 1.4$. Hence in this
 302 model of the leg action, its flexing at transition also helps to keep skis on the snow.
 303 These two scenarios are nicely illustrated by LeMaster (2010) in their Figure 6.3.

304 **Period-amplitude relation.** Since in this model $f(0) = (1-b)^{1/3}$, the small-
 305 amplitude result (18) reads

$$P = 4(1-b)^{1/6} \left(\frac{2\Psi_{max}}{\zeta} \right)^{1/2}. \quad (25)$$

306 Hence, the period of the retractable solution is shorter than the period of the non-
 307 retractable solution by the factor of $(1-b)^{1/6}$. For the reference model, this is about
 308 sixteen percent reduction. The dependence of the period on the amplitude persists in
 309 the nonlinear regime. This is illustrated in Figure 9 for the reference model B with

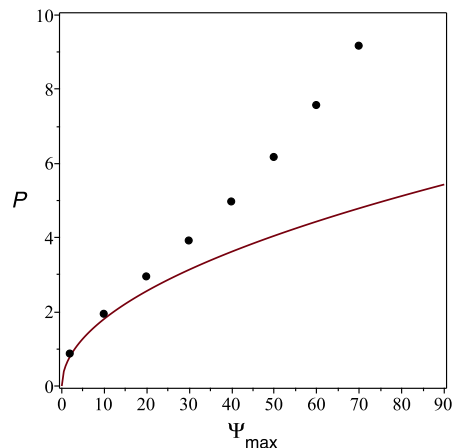


Figure 9. Pendulum period in the reference model B. The line shows the period of the small amplitude solution given by equation (25). The dots show the period of exact solutions found numerically.

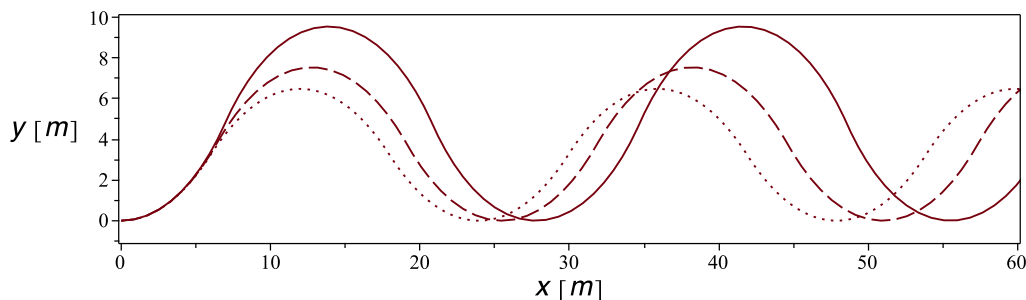


Figure 10. Trajectories of ski runs in the model B with $b = 0$ (solid), $b = 0.6$ (dashed) and $b = 0.8$ (dotted). The other parameters are $l_0 = 1$ m, $R_{sc} = 14$ m, $V = 13.7$ m/s ($\zeta = 1.37$) and $\Psi_{max} = 65^\circ$.

310 $\zeta = 1.2$.

311 The shorter period of solutions with higher retraction parameter b implies
 312 shorter carving turns. This is illustrated in Figure 10 where we present the tra-
 313 jectories corresponding to solutions with $b = 0, 0.6$ and 0.8 . The other param-
 314 eters are fixed to $l_0 = 1$ m, $R_{sc} = 14$ m, $V = 13.7$ m/s and $\Psi_{max} = 65^\circ$. These are chosen
 315 to reflect the values measured in the trial runs studied by Reid (2010).

316 **Scaling with the skier height.** As we discussed at the beginning of this
 317 section, all things being equal, shorter skiers are expected to execute shorter and
 318 straighter (shallower) turns, with the turn length scaling as $\sqrt{l_0}$. In order to illustrate
 319 the scale of this dependence, we simulated the runs made by skiers of the height 202
 320 cm (Ramon Zenhäusern), 180 cm (Alexis Pinturault), and 165 cm (Albert Popov),
 321 thus covering the whole range for current WC slalom racers. As one can see, the

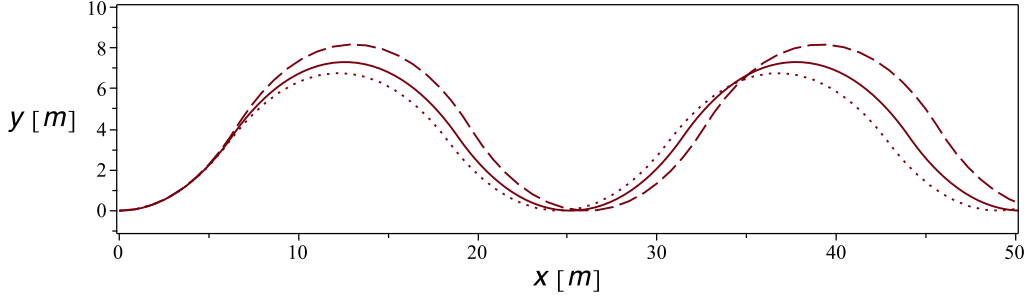


Figure 11. Trajectories of ski runs in the reference corresponding the skier height of 165 cm (dotted line), 180 cm (solid line), and 202 cm (dashed line). The other parameters are $l_0 = 1$ m, $R_{sc} = 14$ m, $V = 13.7$ m/s ($\zeta = 1.37$) and $\Psi_{max} = 65^\circ$.

322 difference in the trajectories is not dramatic but appreciable. In order to compensate
 323 for this effect, shorter skier would have to go for a higher inclination amplitude and/or
 324 higher amplitude of up and down motion (smaller b), making the turn dynamics more
 325 extreme.

326 **Peak ground reaction force.** The results presented in figure 8 suggest that
 327 the peak value of the ground reaction force in the reference model B is not much
 328 reduced compared to the case with fixed leg ($b = 0$). In order to check whether this
 329 conclusion is specific to $\Psi_{max} = 65^\circ$ or not, we used equation (45) of Appendix B to
 330 calculate $F_{GR}^{max} = F_{GR}(\zeta, \Psi_{max})$. This makes sense because the ground reaction force
 331 normally peaks at the extreme position of the pendulum, where $\Psi = \Psi_{max}$. In the
 332 case with fixed leg, the peak value is given by a relatively simple equation,

$$F_{GR,0}^{max} = \zeta \tan \Psi_{max} + \cos \Psi_{max} \quad (26)$$

333 (see Appendix B). The left panel of figure 12 shows F_{GR}^{max} for the reference model
 334 B, whereas the right panel shows its reduction compared to the model with fixed
 335 leg, $\Delta F_{GR}^{max} = F_{GR}^{max} - F_{GR,0}^{max}$. The results confirm that the reduction is indeed rather
 336 marginal, and show that for the combination of high ζ and high Ψ_{max} the ground
 337 reaction force becomes prohibitive. We compare these values with the actual experi-
 338 mental data in the next section.

339 Model versus experimental data

340 With the snow contact issue resolved, it makes sense to carry out a somewhat
 341 more detailed check of the pendulum model against the data obtained in experimental
 342 studies of turn dynamics in ski racing. This should help to evaluate its current fitness
 343 and to identify the ways of further development. In this section, we pay particular
 344 attention to the magnitude of the ground reaction force which skiers face during
 345 carving turns .

346 Figure 13 shows the predicted peak value of the ground reaction force as a
 347 function of the maximum inclination angle Ψ_{max} and the speed parameter ζ . One

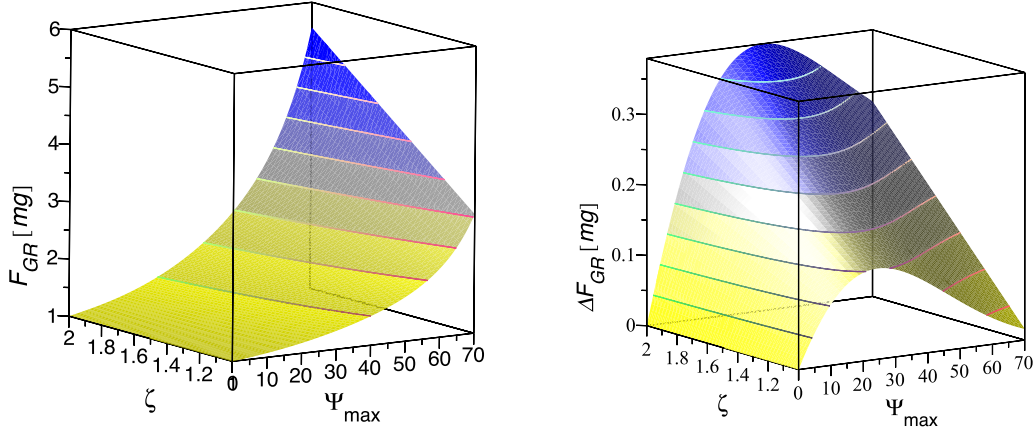


Figure 12. *Left panel:* Peak value of the ground reaction force in the reference model B as a function of the speed parameter ζ and the pendulum amplitude Ψ_{max} . *Right panel:* The reduction of the peak value compared to case with fixed leg. The results are given in the units of mg .

348 can see that the model A, where the pendulum load remains at the same height
 349 throughout its oscillations, yields noticeably lower ground reaction force than the
 350 model B, where the load lowers on approach to the turning point.

351 It is interesting to compare the model predictions with the actual parameters
 352 of turns performed by elite athletes. In table 1 we list the maximum speed V_{max} , the
 353 shortest local turn radius R_{min} and the peak ground reaction force $F_{GR,max}$ recorded in
 354 the field studies of Gilgien et al. (2014) and (Reid, 2010). The data for giant slalom
 355 (GS), super-giant slalom (SG) and downhill (DH) is based on the runs made by
 356 forerunners of the World Cup competitions during the 2010/11 and 2011/12 seasons
 357 (Gilgien et al., 2014). Only the data from the turns with the 10% most extreme
 358 values was included in their statistical analysis. It is not possible to say if the peak
 359 values of these parameters correspond to the same turn or to different turns. In fact,
 360 in ski racing the skier speed is often higher on flatter parts of a race track whereas
 361 the turn radius is often smaller on its steeper sections (Gilgien, Crivelli, Spörri, Kröll,
 362 & Müller, 2015). The data for GS, SG and DH is simply copied from the table 2 in
 363 Gilgien et al. (2014). This paper gives no information on the sidecut radius of skis
 364 used in the trials. For this reason, we had to adopt the minimum radius allowed by
 365 the FIS regulations for the 2010/2011 season. This should be a reasonably good guess
 366 as racers tend to prefer skis with the smallest allowed sidecut radius.

367 The slalom (SL) data is based on the trial runs made by members of Norwegian
 368 national Europa Cup team of the 2005/2006 season. This study used a carefully
 369 selected slope which provided uniform conditions throughout a course and courses

Table 1

Parameters of the trail runs studied in Gilgien et al. (2014) and Reid (2010) and the corresponding parameters of the pendulum model. R_{sc} is the assumed ski sidecut radius. $\langle V \rangle$, V_{max} , R_{min} , and $F_{GR,max}$ are respectively the mean turn speed, the top speed, the lowest local turn radius, and the top ground reaction force measured during the trials. ζ is the speed parameter of the pendulum model corresponding to $\langle V \rangle$ (for the SL data) or V_{max} (for the GS, SG and DH data) and R_{sc} ; Ψ_{max} is the maximum inclination angle corresponding to R_{sc} and R_{min} as prescribed by the Howe formula (Howe, 1983); $F_{GR,A}$ and $F_{GR,B}$ is the ground reaction force in the pendulum model expected for the leg retraction models A and B and given in the units of mg.

Parameter	SL	GS	SG	DH
R_{sc}	14 m	27 m	33 m	45 m
$\langle V \rangle$ or V_{max}	13.7 m/s	22.2 m/s	28.3 m/s	32.3 m/s
R_{min}	6 m	8.4 m	17.2 m	20.6 m
F_{GR}^{max}	3.2	3.16	2.79	2.59
ζ	1.37	1.86	2.47	2.36
Ψ_{max}	65°	71.8°	58.6°	62.7°
$F_{GR,A}^{max}$	2.37	3.20	1.92	2.18
$F_{GR,B}^{max}$	3.23	5.73	4.11	4.62

370 that promoted repetitive rhythmic skiing with minimal differences between turns.
371 This was done with the aim of accumulating a set of data which was sufficiently large
372 for a robust statistical analysis of the kinematics and dynamics of a typical slalom
373 turn (Reid, 2010). We extracted the data shown in table 1 from figures 6.3, 6.6, 6.10,
374 and 6.32 in Reid (2010) using a basic ruler. Each figure shows the mean value of a
375 displayed parameter and its standard deviation as a function of the turn phase. We
376 used only the mean value curves to determine the turn parameters given in table 1.
377 In particular, $\langle V \rangle$ is defined as an arithmetic mean of the highest and lowest values of
378 the curve for the outside ski speed. R_{min} is the lowest value of the curve for the local
379 turn radius of outside ski, and $F_{GR,max}$ is the highest value of the curve for the ground
380 reaction force. Although these are reached not at exactly the same turn phase, the
381 difference between the phases is not that great. In addition, Reid (2010) present two
382 separate sets of data, for race courses which had different gate separation. In table 1,
383 we give an arithmetic mean of the numbers found for these two sets. Reid (2010) do
384 not explicitly state the sidecut radius of trial skis but for their calculations they use
385 a model with $R_{sc} = 14$ m. So we expect this to be the typical radius of skis in their
386 trials.

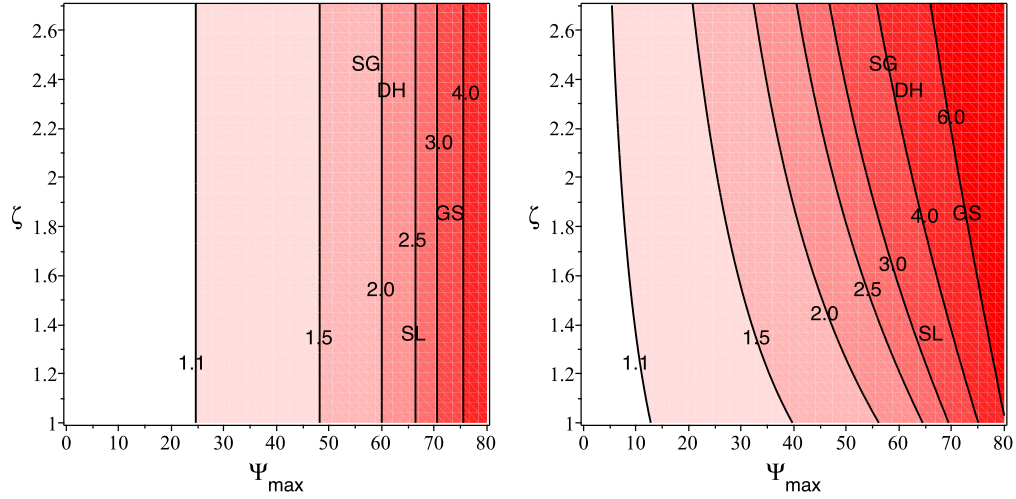


Figure 13. Peak ground reaction force in the reference models A (left panel) and B (right panel) as a function of the speed parameter ζ and the pendulum amplitude Ψ_{max} . We also show the positions corresponding in these models to the peak parameters of the racing runs measured in Gilgien et al. (2014) and Reid (2010).

387 We use the values of $\langle V \rangle$ (for the SL data) or V_{max} (for the GS, SG, and DH
 388 data) and R_{sc} to calculate the values of the speed parameter ζ , using equation (2),
 389 and the values of R_{sc} and R_{min} to calculate the ski inclination angle, Ψ_{max} , using
 390 equation (5). Finally, the determined values of ζ are fed into equations (45) and
 391 (44) to find the corresponding peak values of the snow reaction force expected in the
 392 leg-retraction models A and B. The results are presented in table 1 and in figure 13.

393 The most encouraging conclusion that follows from results presented in table 1
 394 is that the peak ground reaction force predicted by the pendulum model for slalom
 395 runs using the leg retraction model B is almost identical to the snow reaction force
 396 measured in Reid (2010). This is particularly impressive because in this case the
 397 model has no free parameters which could be used for fine tuning. Indeed, 1) the
 398 retraction model is chosen via fitting the actual variation of the CM height (figure 6.21
 399 in Reid (2010)), 2) the speed parameter ζ is fixed by the measured ski speed and their
 400 sidecut radius, 3) the oscillation amplitude Ψ_{max} is fixed by the observed minimum
 401 turn radius and the sidecut radius of skis, and 4) there are no other parameters in
 402 the model.

403 For more detailed comparison with the experimental data we have prepared plots
 404 showing the evolution of the CM height h , local turn radius R , the ski inclination
 405 angle Ψ and the ground reaction force F_{GR} (see figure 14). These are to be compared
 406 with figures 6.21, 6.6, 6.10, and 6.32 in Reid (2010) respectively. The data provide two
 407 additional quick checks for the model. Firstly, the experimental data give $\Psi_{max} \approx$
 408 67° , which is not far from the theoretical value of $\Psi_{max} = 65^\circ$, indeed. Secondly,
 409 the experimental minimum value for the ground reaction force during the transition

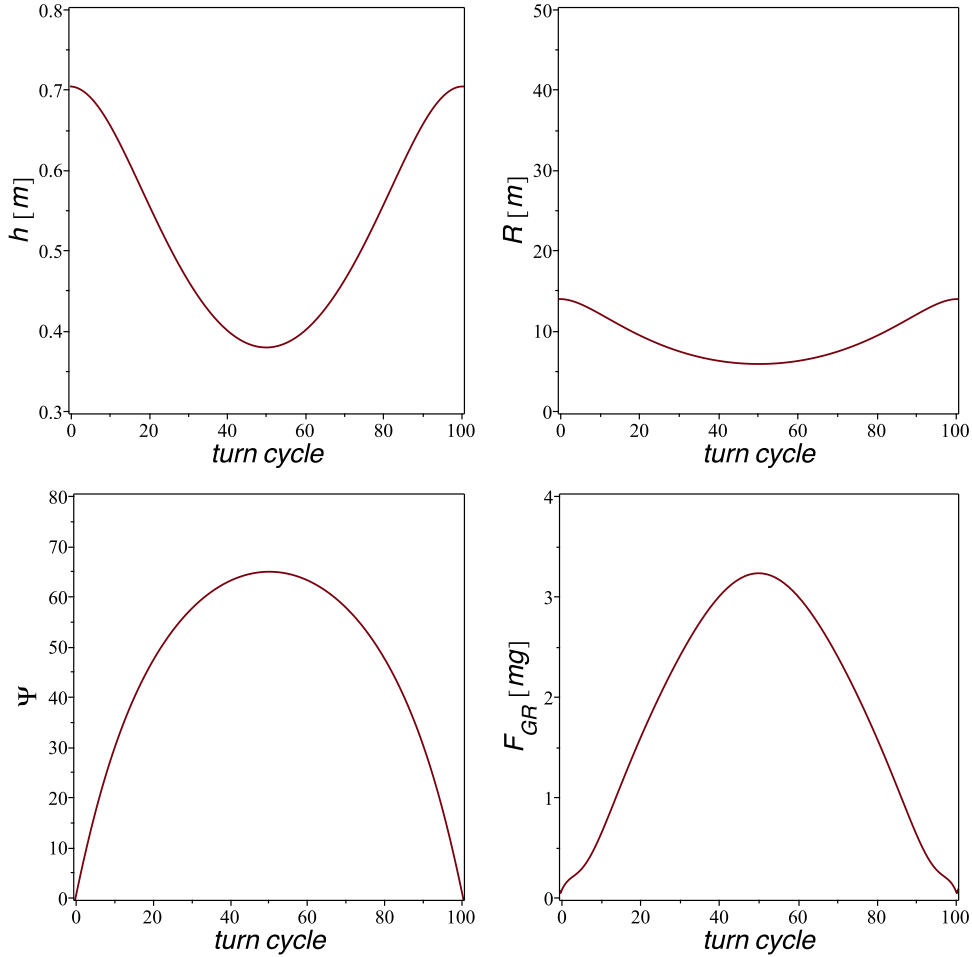


Figure 14. Pendulum CM height above the ground, local turn radius, inclination angle and ground reaction force as a function of the turn cycle (in %) in the reference model B with $l_0 = 1$ m, $R_{sc} = 14$ m, $\zeta = 1.37$, and $\Psi_{max} = 65^\circ$.

410 between turns, $F_{GR,min} \approx 0.25 mg$, which is also similar to what is seen in figure 14.
 411 Ignoring the sudden dive at the exact boundary, we find $F_{GR,min} \approx 0.2 mg$.

412 The comparison also reveals some notable differences. The most noticeable one
 413 is the high local turn radius observed in the experimental data for up to 30 percent
 414 of the turn cycle, in the transition phase. During this period, the turn radius can
 415 strongly exceeds the ski sidecut radius, implying that skis are not carving. Not only
 416 skis but also the skier CM has a much more straightened trajectory during this phase,
 417 suggesting an almost inertial motion. This conclusion is supported by a noticeably
 418 longer phase of low ground reaction force in the experimental data. In fact, it is
 419 common knowledge that skidding and pivoting of skis in transition between turns is
 420 an essential part of slalom technique.

421 Figure 15 shows the ski trajectory predicted in model B using the parameters

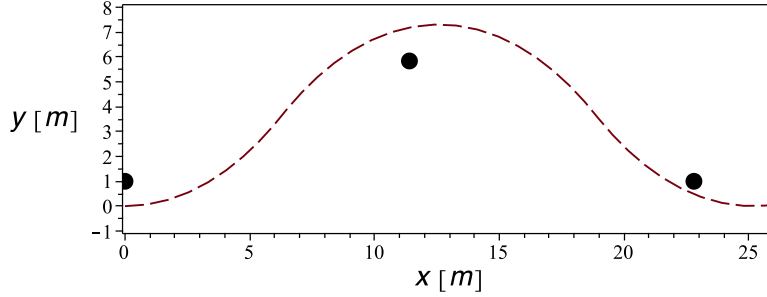


Figure 15. Theoretical ski trajectory predicted in the reference model B versus the gate positioning in Reid (2010). The model parameters are $R_{sc} = 14$ m, $l_0 = 1$ m, $\zeta = 1.37$ and $\Psi_{max} = 65^\circ$. The distances between turning poles are $\Delta x = 11.4$ m and $\Delta y = 4.84$ m.

422 from table 1 and the position of turning poles as in Reid (2010). Like with other
 423 data, we used the arithmetic mean of the distances for the two courses they set. The
 424 theoretical turn is a bit longer and wider than needed, with skis clearing the gates
 425 with about one meter margin, but given the model simplifications we see this as a
 426 reasonable agreement.

427 As to the results for GS, SG and DH presented in table 1, it is obvious that for all
 428 these disciplines, the leg retraction model B predicts peak values of the snow reaction
 429 force which significantly exceed the experimental values and could be unbearable.
 430 Moreover, we have found that in all the three cases the model predicts a loss of snow
 431 contact in transition between turns. It could be that V_{max} is measured in one turn
 432 and R_{min} in a completely different turn and may be even on a completely different
 433 section of the race track. In this case, its possible that in any individual turn the
 434 combination of ζ and Ψ_{max} is less extreme, resulting in a lower ground reaction force
 435 and a weaker catapulting effect at the end of the turn.

436 For the model A the predicted peak values of the ground reaction force are closer
 437 to the experimental values. In fact, for GS they are almost identical. However, the
 438 deduced inclination angle Ψ_{max} exceeds the limiting value $\Psi_{lim} \approx 60^\circ$ of this model.
 439 This value of Ψ_{max} corresponds to a 200% increase in the distance between the skier
 440 CM and the ski base during the turn, which likely would require skiers to press their
 441 knees against their chest at the transition between turns.

442 For SG and DH the deduced values of Ψ_{max} are approximately equal to Ψ_{lim} ,
 443 making the model A a more realistic possibility. However, the ground reaction force
 444 predicted in this model is significantly below the observed values. This suggests that
 445 in the speed disciplines, the height of skier's CM is still variable, but to a lesser extent
 446 than in slalom. Although this seems to agree with our naked eye inspection of many
 447 openly available video records of WC races, a proper quantitate analysis is required.
 448 Overall, the results are not conclusive and more detailed experimental studies of turn
 449 kinematics in these disciplines, similar in rigour to Reid (2010), are required for a

450 more informative analysis.

451 Since the issue of snow reaction force is important for prevention of injuries,
 452 which trouble the sport, we finish this section by explaining why the model A provides
 453 a substantial reduction for the peak values of this force during the turn. At first glance
 454 this is rather odd, as for the same speed and the same inclination angle in both models
 455 the skier experiences exactly the same centrifugal and gravity forces. However, our
 456 simple pendulum model shows that the ground reaction force is also influenced by
 457 the leg action, by how fast it is extended and contracted during its swing. This is
 458 already evidenced by equations (6) and (7). At the extreme position ($\Psi = \Psi_{max}$),
 459 $d\Psi/dt = 0$ and the radial acceleration of the pendulum load reduces to

$$a_r = \frac{d^2l}{dt^2}. \quad (27)$$

460 As in both models l increases with Ψ , we have $a_r < 0$ at Ψ_{max} and hence the ground
 461 reaction force is reduced via the leg action. However, in the model A this effect is
 462 stronger. In order to understand why, let us consider all forces acting on the load at
 463 $\Psi = \Psi_{max}$. In the model A, the vertical component of the leg reaction force W_{\perp} must
 464 balance the gravity force in order to preserve constant load height above the ground.
 465 Hence, $W_{\perp} = mg$ and the total leg reaction force

$$W = mg(1 + \tan^2 \Psi_{max})^{1/2}, \quad (28)$$

466 just because its vector is aligned with the leg (see figure 1). In the model B, the load
 467 height increases after the turning point and hence the vertical component of \mathbf{W} must
 468 be higher by $\delta W_{\perp} = ma_{\perp}$ where a_{\perp} is the vertical acceleration of the load. For high
 469 Ψ_{max} , the corresponding increase of the total reaction force,

$$\delta W = \delta W_{\perp}(1 + \tan^2 \Psi_{max})^{1/2}, \quad (29)$$

470 can be much higher than δW_{\perp} . In the model corresponding to the trial runs in Reid
 471 (2010), the total variation of the CM height $\Delta h = 0.33$ m. Assuming that for one half
 472 of this distance the vertical acceleration is positive, one can estimate its magnitude via
 473 the standard equation for the distance covered from rest under constant acceleration,

$$a_{\perp} = \frac{\Delta h}{T^2}, \quad (30)$$

474 where T is the time required to reach the height $\Delta h/2$. This time should be about one
 475 quarter of the whole turn duration. Given the length of the simulated turn $L \approx 14$ m
 476 (c.f. figure 15) and the ski speed $V = 13.7$ m/s, we estimate $T \approx 0.25$ s and hence
 477 $a_{\perp} \approx 0.5g$, which is not far from the value of $0.37g$ found in our numerical simulations.
 478 For $\Psi_{max} = 65^\circ$, this corresponds to $\delta W = 1.12 mg$, which is not far from the actual
 479 difference between the reaction forces in the models A and B (see table 1).

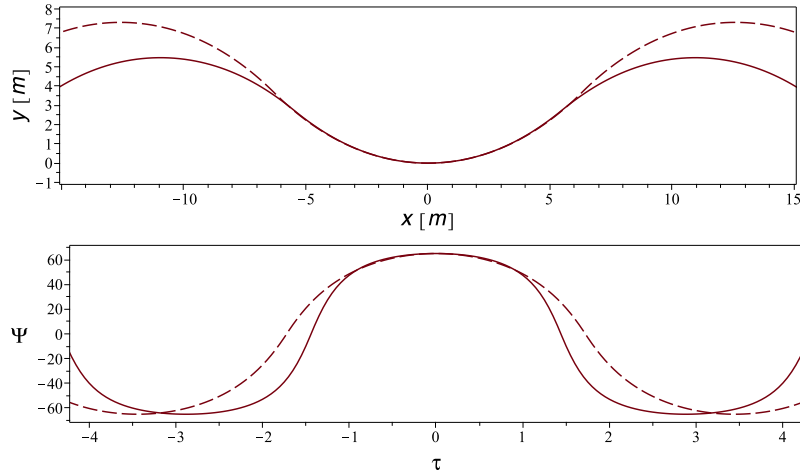


Figure 16. *Top panel:* Ski trajectories in the reference models A (solid line) and B (dashed line) for the same run parameters: $l_0 = 1$ m, $R_{sc} = 14$ m, $V = 13.7$ m/s, and $\psi_{max} = 65^\circ$. *Bottom panel:* The corresponding variation of the inclination angle.

480 In skiing terms, the model A corresponds to a faster extension of skier's legs
 481 (mainly their outside leg) on approach to the turning point and a faster flexion of the
 482 legs after passing this point, compared to the model B. The faster flexion means that
 483 the skier A offers lesser resistance to the compression coming from the snow. Based
 484 on this interpretation, one would expect a smaller impulse received by this skier in the
 485 direction normal to the overall direction of travel and hence shallower turns. In figure
 486 16 we compare the ski trajectories in the models A and B for the same parameters as
 487 in figure 15. In agreement with our expectation, in the model A the turns are indeed
 488 shallower and shorter. Interestingly, the shapes of turn arcs are very much the same
 489 in both the cases but the speed of transition from arc to arc is noticeably faster in
 490 the model A. This can also be seen in the plots of $\Psi(\tau)$, presented in the lower panel
 491 of figure 16.

492 Discussion and Implications

493 In this study we aimed to learn more about the potential of the centrifugal
 494 pendulum model in capturing essential features of carving turns in expert skiing and
 495 racing. The main focus was on how to prevent the loss of snow contact at high speed
 496 ($\zeta > 1$) predicted by the basic pendulum model. Indeed, this prediction is in conflict
 497 with the skiing practice as $\zeta > 1$ is typical for racing and yet racers manage to avoid
 498 being catapulted into the air. The main advice given by ski coaches in this regard is to
 499 flex legs in transition between turns and to extend them during turns, the technique
 500 analogous to that used in bump skiing for the same reason. Based on this advice, we
 501 advanced the pendulum model by allowing variation of its length during oscillations.

502 The introduction of leg retraction function made the structure of differential

503 equations governing the pendulum motion a little bit more complex, but a number of
504 its important properties remain unchanged. In particular, it has the same qualitative
505 dependence on the speed parameter ζ . Like in the basic model, for $\zeta < 1$ the pendu-
506 lum has three equilibrium solutions, and for $\zeta > 1$ these equilibria do no longer exist.
507 This conclusion does not depend on the specific form of the leg retraction function.
508 In application to skiing it means that the leg action does not effect the value of the
509 critical speed above which carving turns become incompatible with lateral balance
510 between the gravity, centrifugal and snow reaction forces.

511 Like in the basic model (Komissarov, 2020), the period of pendulum oscilla-
512 tions depends on their amplitude, even in the small amplitude limit, with a smaller
513 amplitude leading to a shorter period. In skiing this implies that reduction of skier
514 inclination during turns results in them becoming shorter and shallower.

515 Similarly to the basic model, the pendulum period increases with the length
516 of its leg (Komissarov, 2020). In application to skiing this means that, given the
517 same equipment, shorter skiers will tend to make shorter turns compared to taller
518 skiers. To compensate for this, they may be forced to go for more extreme inclination,
519 which increases the turn duration. In agreement with this general period dependence
520 on the pendulum length, we find that contraction of the pendulum leg near the
521 vertical position reduces the oscillation period compared to the case where it remains
522 unchanged (the same as in the extreme position). In skiing this implies that leg flexion
523 in transition between turns makes them shorter, both in duration and in length.

524 In our numerical modelling, we probed the effect of leg flexion on the snow
525 contact in transition between carving turns using two specific models of this leg
526 action. In our approach we did not aim at building a flexible model which could
527 be used to reproduce the exact action of real skiers, which varies from individual
528 to individual and depends on a number of external factors. Instead, we wanted a
529 relatively simple model which could be easy to implement and analyse.

530 In the first example (case A) the pendulum load remains at the same height
531 above the ground throughout its oscillation. In skiing this corresponds to such an
532 execution of ski turns that the height of skier's CM above the snow remains invariant
533 throughout a turn. This implies that 1) the vertical component of the leg reaction
534 force applied to the pendulum load always balances the vertical component of gravity
535 force, and 2) the radial component of the ground reaction force at the pivot is always
536 positive. In other words, the pivot is always pushed into the ground. Thus, the setup
537 automatically ensures that the snow contact issue never emerges. We note that in
538 this case, the ground reaction force does not reduce below mg when the pendulum
539 goes through the vertical position. In skiing this implies that such leg action is
540 incompatible with pivoting of skis in transition between turns, which requires skis to
541 be unloaded. However in pure carving such pivoting of skis is completely eliminated,
542 and instead they are simply rolled from one edge to another.

543 Remarkably, the total ground reaction force corresponding to this leg action
544 does not depend on the speed parameter ζ or the amplitude of pendulum oscillations

545 Ψ_{max} , but is completely determined by the skis (and hence skier) inclination angle.
 546 Moreover, for inclination angles $\Psi < 60^\circ$ the ground reaction force stays rather low,
 547 $F_{GR} < 2mg$. At first glance, the lack of dependence on ζ seems to suggest a possibility
 548 of turning at extremely high speeds without encountering prohibitively large forces.
 549 However as the speed increases, the skier trajectory approaches a straight line, with
 550 skis moving from side to side only by the distance dictated by the length of skier's
 551 legs and their inclination.

552 One important limitation of this leg action concerns achievable inclination an-
 553 gles. The model has an upper limit on these angles which is dictated by the lowest
 554 anatomically possible height of skiers CM above the snow in transition between turns.
 555 We estimate this height as approximately 50 percent of the CM height in maximally
 556 extended upright position (which is about 100 cm for a 180 cm tall skier). The cor-
 557 responding limit on the inclination angle is $\Psi_{lim} = 60^\circ$. Although this limit is not
 558 low, even more extreme inclinations are often used by top athletes (e.g. see table 1).
 559 In addition, skiers do use up and down motion to control the tilt of their skis and
 560 hence the turn radius.

561 In the second example (case B), the pendulum load is allowed to move up and
 562 down to a degree controlled by its single parameter b . For $b = 0.65$ the amplitude of
 563 this movement is very close to the one observed in slalom turns by (Reid, 2010). In
 564 fact, it is noticeably lower than that in the pendulum with fixed leg length, and our
 565 calculations show that this has a strong effect on the ground reaction force experienced
 566 by the pendulum when it passes its vertical position. For a large section of the
 567 parameter space where in the model with fixed leg the pendulum pivot is pulled away
 568 from the ground, in the model B it can be still pushed against it. In application to
 569 skiing this implies that skis can be kept in snow contact throughout the whole turn
 570 cycle. In particular for the parameters of the trial runs described in Reid (2010), the
 571 model B predicts $0 < F_{GR} \lesssim 0.25 mg$, which is in a good agreement the actual data
 572 (Reid, 2010). Since $F_{GR} \ll mg$, the skis are not pressed against the snow as much
 573 as in a stationary position and this “unweighting” of skis facilitates their pivoting at
 574 transition between turns, which is a typical element of turn technique in slalom.

575 As to the peak value of the ground reaction force, which is experienced at the
 576 extreme pendulum position ($\Psi = \Psi_{max}$), we find that it is only marginally reduced
 577 compared to the case with fixed pendulum leg. For the parameters of the trial runs
 578 set by Reid (2010), the reference model predicts $F_{GR}^{max} \approx 3.2 mg$, which is also in
 579 a very good agreement with the experimental data. In fact, the reference model B
 580 allows to reproduce all basic parameters of the SL runs studied in Reid (2010) quite
 581 well. Even the predicted ski trajectory provides a reasonable fitting of their course
 582 setting.

583 Our comparison of the predicted snow reaction force in models A and B shows
 584 that the model A allows a substantial reduction of its peak value compared to the
 585 model B and suggests that minimisation of the CM height variation during skiing turns
 586 can help to reduce the risk of leg injury (cf. Gilgien et al., 2014). The reason behind

587 the difference is due to the additional push against the snow required in the model B
588 in order to initiate the accelerated upward motion of the CM from its lowest position.
589 This additional force increases with the skier inclination angle simply because it has
590 the same inclination and hence must increase in order to support the same vertical
591 acceleration.

592 We tested the models against the data for GS, SG and DH in Gilgien et al.
593 (2014), who give extreme values of speed, turn radius and snow reaction force en-
594 countered in their experiments. Assuming that these apply to a single most extreme
595 turn of their runs, we find that the reference model B overpredicts the peak ground
596 reaction force in speed disciplines, whereas the reference model A underpredicts them.
597 This suggests up and down motion of skiers' CM but to a lesser degree than in slalom.
598 However, more detailed experimental data is needed to reach reliable conclusions.

599 There is no doubt that the pendulum model is an extremely simplified repre-
600 sentation of skiers and their equipment. The human body is much more complex
601 with many degrees of freedom. There is an understandable temptation to build
602 multi-component Hanavan-like models, where both the skier and their equipment
603 are represented by many segments connected by mechanical joints and hope that
604 the power of modern computers will allow to run realistic simulations of skiing (e.g.
605 Oberegger, Kaps, Mössner, Heinrich, & Nachbauer, 2010; Roux, Dietrich, & Doix,
606 2010). However, in such models one would inevitably face the problem of dealing
607 with highly multi-dimensional phase space. Such problems are computationally very
608 expensive and it is not clear how much can be learned this way. In order to explore
609 the parameter space, it will not be sufficient to run just several simulations. Many
610 more would be needed to allow for optimisation. It will also be difficult to interpret
611 results, to separate key factors from unimportant ones.

612 The more traditional route of theoretical science is to start from a simple math-
613 ematical model including a rather limited number of factors, which are expected to
614 be most important according to current paradigm or practice. Once their role is fully
615 understood, and if the model is found insufficiently realistic, more factors can be in-
616 cluded. Our pendulum model is an example of this approach. The good agreement
617 between this model and the experimental studies of slalom turns (Reid, 2010) shows
618 that, in spite of its simplicity, the pendulum model is a useful tool for analysing the
619 dynamics of alpine skiing.

620 In addition to the leg flexion and extension, there is a number of other aspects
621 of alpine skiing that can be explored using the pendulum model. One aspect which
622 we hope to explore in a foreseeable future is the skier angulation, which makes the
623 ski tilt differ from the CM tilt. This technical element is widely used and considered
624 quite important. For example according to the study by Reid (2010), in slalom turns
625 the CM tilt can be up to 20° smaller than the ski tilt. Such a large difference can
626 have a noticeable effect on the turn dynamics.

627 Another possible topic is the role of the inside ski/leg. Indeed, in contrast to
628 the pendulum, skiers have two legs, and in modern skiing they are kept well apart

629 and do not perform as a single unit. In fact, when legs extend during the turn phase,
 630 the inside leg extends less compared to the outside one and may even flex (e.g. Harb,
 631 2006; LeMaster, 2010). One may argue that the pendulum leg corresponds to the
 632 outside skier leg (the leg which is further away from the centre of turn's arc) because
 633 it normally bears most of the load. Since in transition between skiing turns the
 634 outside skier leg becomes the inside one and the other way around, for the pendulum
 635 with one leg this implies a horizontal shift of its pivot, which can be easily included
 636 in the model. A similar shift seems to occur during pivoting of unweighted skis in
 637 slalom turns. A next step could be developing a model for a pendulum with two legs.

638 Conclusion

639 In this paper we advanced the model of centrifugal pendulum by allowing vari-
 640 ation of pendulum length during swinging. This has allowed us to test the hypothesis
 641 that such a variation may help to overcome the limitations of the basic model with
 642 fixed leg which predicts a loss of snow contact in transition between turns at high
 643 speeds characteristic to ski racing. In particular, we have found that leg flexion on
 644 approach to the summit point is a very efficient way of preserving the snow contact,
 645 in agreement with the practice of ski racing. We have also found that restriction of
 646 the up and down motion of skier's centre of mass during turns can allow a substan-
 647 tial reduction of the peak ground reaction force, and hence reduce the risk of injury.
 648 Our check of the model against the available data on rhythmic slalom turns made
 649 by professional athletes shows a good agreement and allows us to conclude that the
 650 model is a very useful tool for deciphering the complicated dynamics of skiing.

651 Acknowledgments

652 All non-trivial calculations of this study were carried out with the software
 653 package *Maple* (Maple is a trademark of Waterloo Maple Inc.).

Appendix A

Energy of the centrifugal pendulum

654 It is not very difficult to verify that the Lagrangian of the dynamical system described
 655 by equation (11) is

$$L(\dot{\Psi}, \Psi) = \frac{1}{2}f^4\dot{\Psi}^2 - U(\Psi), \quad (31)$$

656 where $\dot{\Psi} = d\Psi/d\tau$ and

$$U(\Psi) = - \int f^3(\Psi)(\sin \Psi - \zeta \operatorname{sgn}(\Psi))d\Psi \quad (32)$$

657 is the potential energy. The conserved total energy of the pendulum is

$$E = \dot{\Psi} \frac{\partial L}{\partial \dot{\Psi}} - L = \frac{1}{2}f^4(\Psi)\dot{\Psi}^2 + U(\Psi). \quad (33)$$

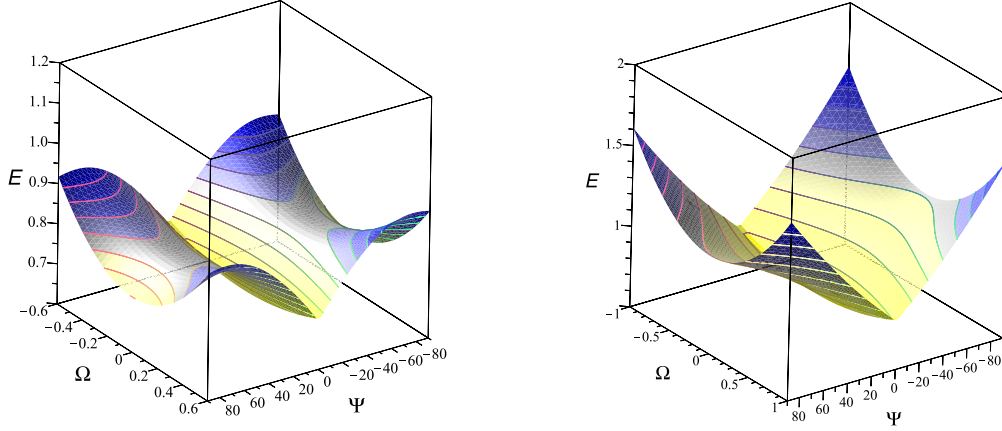


Figure A1. Energy of the pendulum in model B with $b = 0.65$ for $\zeta = 0.8$ (left) and $\zeta = 1.2$ (right).

658 Since at the turning point $\dot{\Psi} = 0$ and $\Psi = \Psi_{max}$ we have $E = U(\Psi_{max})$.

659 For $f(\Psi) = (1 - b \cos \Psi)^{1/3}$ equation (32) yields

$$U(\Psi) = -\frac{b}{2} \cos^2 \Psi + \cos \Psi + \zeta (-b |\sin \Psi| + |\Psi|) \quad (34)$$

660 Figure A1 shows the total energy for $b = 0.65$ and $\zeta = 0.8, 1.2$. In both cases it has
 661 a minimum at $(\Psi, \Omega) = (0, 0)$, corresponding the vertical equilibrium of the pendu-
 662 lum. When $\zeta = 0.8$ the function has two saddle points at $(\Psi, \Omega) = (\pm \arcsin(\zeta), 0)$,
 663 corresponding to the two inclined equilibria of the system.

664 For $f(\Psi) = 1/\cos \Psi$ we have

$$16U(\Psi) = -\frac{1}{\cos^2 \Psi} + \zeta \operatorname{sgn} \Psi (\sec \Psi \tan \Psi + \ln(\sec \Psi + \tan \Psi)) . \quad (35)$$

Appendix B

Ground reaction force

665 The radial motion of the pendulum mass m is described by the equation

$$ma_r = F_{GR} + (\mathbf{F}_c + \mathbf{F}_g) \cdot \mathbf{i}_r , \quad (36)$$

666 where a_r is the radial acceleration, \mathbf{F}_c and \mathbf{F}_g are the centrifugal and gravity forces
 667 respectively (see equations 3 and 4), $\mathbf{i}_r = \sin \Psi \mathbf{j} + \cos \Psi \mathbf{k}$ is the unit vector in the
 668 radial direction and W is the ground reaction force at the pivot point. Substituting
 669 the expressions for the gravity and centrifugal forces into (36), we find that in the
 670 units of mg

$$F_{GR} = \zeta |\tan \Psi| + \cos \Psi + \frac{a_r}{g} . \quad (37)$$

671 The radial acceleration

$$a_r = \frac{d^2 l}{dt^2} - l \left(\frac{d\Psi}{dt} \right)^2 = l_0 \left(\frac{d^2 f}{dt^2} - f \left(\frac{df}{dt} \right)^2 \right) = g(\ddot{f} - f\dot{f}^2). \quad (38)$$

672 Since $\dot{f} = f'\dot{\Psi}$ and $\ddot{f} = f''\dot{\Psi}^2 + f'\ddot{\Psi}$, we have

$$\frac{a_r}{g} = (f'' - f)\dot{\Psi}^2 + f'\ddot{\Psi}. \quad (39)$$

673 Using the pendulum equation (11) we find that

$$\ddot{\Psi} = -2 \frac{f'(\Psi)}{f(\Psi)} \dot{\Psi}^2 + \frac{\sin(\Psi) - \zeta \operatorname{sgn}(\Psi)}{f(\Psi)} \quad (40)$$

674 Substituting this expression into (39) and hence substituting the result into (37), we
675 finally obtain

$$F_{GR} = \zeta |\tan \Psi| + \cos \Psi + \frac{f'}{f} (\sin \Psi - \zeta \operatorname{sgn} \Psi) + \left(f'' - \frac{2f'^2}{f} - f \right) \dot{\Psi}^2. \quad (41)$$

676 Since the energy equation (33) yields

$$\dot{\Psi}^2 = \frac{2}{f^4(\Psi)} (U(\Psi_{max}) - U(\Psi)), \quad (42)$$

677 the ground reaction force is a function of Ψ , its amplitude Ψ_{max} , the speed parameter
678 ζ and whatever parameters enter the expression for the retraction function $f(\Psi)$.

679 In the case with fixed leg, $f' = f'' = 0$ and (41) reduces to

$$F_{GR,0} = \zeta |\tan \Psi| + \cos \Psi - f \dot{\Psi}^2. \quad (43)$$

680 For $f = 1/\cos \Psi$, the last term in equation (41) vanishes, $f'/f = \tan \Psi$ and hence

$$F_{GR} = \frac{1}{\cos \Psi}. \quad (44)$$

681 In this special case, the ground reaction force does not depend on the speed parameter
682 ζ and the oscillation amplitude Ψ_{max} .

683 At the turning point $(\Psi, \dot{\Psi}) = (\Psi_{max}, 0)$, and (41) reduces to

$$F_{GR}^{max} = \zeta \tan \Psi_{max} + \cos \Psi_{max} + \frac{f'(\Psi_{max})}{f(\Psi_{max})} (\sin \Psi_{max} - \zeta \Psi_{max}). \quad (45)$$

684 For the case with fixed leg, this equation yields

$$F_{GR,0}^{max} = \zeta \tan \Psi_{max} + \cos \Psi_{max}. \quad (46)$$

References

685

- 686 Davidovits, P. (2018). *Physics in biology and medicine*. Cambridge, Massachusetts: Aca-
687 demic Press.
- 688 Domire, Z., & Challis, J. (2007). The influence of squat depth on maximal vertical jump
689 performance. *Journal of Sports Sciences*, 25(2), 193-200.
- 690 Gilgien, M., Crivelli, P., Spörri, J., Kröll, J., & Müller, E. (2015). Characterization of
691 course and terrain and their effect on skier speed in world cup alpine ski racing. *PLoS*
692 *ONE*, 10, e0118119.
- 693 Gilgien, M., Spörri, J., Kröll, J., Crivelli, P., & Müller, E. (2014). Mechanics of turning
694 and jumping and skier speed are associated with injury risk in men's world cup alpine
695 skiing: a comparison between the competition disciplines. *British Journal of Sports*
696 *Medicine*, 48, 742-747.
- 697 Harb, H. (2006). *Essentials of skiing*. New York: Hatherleigh Press.
- 698 Hetherington, G. (2016). *Most important move in skiing (part 1): Alltracks academy*.
699 Retrieved from www.youtube.com/user/AlltracksAcademy/videos
- 700 Howe, J. (1983). *Skiing mechanics*. Laporte, Colorado: Poudre Press.
- 701 Jentschura, U., & Fahrbach, F. (2004). Physics of skiing: The ideal carving equation and
702 its applications. *Canadian Journal of Physics*, 82, 249-261.
- 703 Komissarov, S. (2018). *Modelling of carving turns in alpine skiing*. (SportRxiv.
704 <https://doi.org/10.31236/osf.io/u4ryc>)
- 705 Komissarov, S. (2020). Dynamics of carving turns in alpine skiing: I: The basic centrifugal
706 pendulum. *Sports Biomechanics*, 25(2), 193-200.
- 707 Landau, L., & Lifshitz, E. (1969). *Mechanics*. Oxford: Pergamon Press.
- 708 LeMaster, R. (2010). *Ultimate skiing*. Champaign: Human Kinetics.
- 709 Lind, D., & Sanders, S. (1996). *The physics of skiing: Skiing at the triple point*. New York:
710 Springer-Verlag.
- 711 Morawski, J. (1973). Control systems approach to a ski-turn analysis. *Journal of Biome-*
712 *chanics*, 6, 267-279.
- 713 Oberegger, U., Kaps, P., Mössner, M., Heinrich, D., & Nachbauer, W. (2010). Simulation
714 of turns with a 3d skier model. *Procedia EnginFeering*, 2(2), 3171-3177.
- 715 Reid, R. (2010). *A kinematic and kinetic study of alpine skiing technique in*
716 *slalom* (PhD dissertation, Norwegian School of Sport Sciences). Retrieved from
717 <http://hdl.handle.net/11250/171325>
- 718 Reid, R. C., Haugen, P., Gilgien, M., Kipp, R. W., & Smith, G. A. (2020). Alpine ski
719 motion characteristics in slalom. *Frontiers in Sports and Active Living*, 2, 25-36.
- 720 Roser, M., Appel, C., & Ritchie, H. (2020). "human height". *"Our World in Data"*. Retrieved
721 from <https://ourworldindata.org/human-height>
- 722 Roux, F., Dietrich, G., & Doix, A.-C. (2010). Skier-ski system model and de-
723 velopment of a computer simulation aiming to improve skier's performance and
724 ski. In *Proceedings of the 1st augmented human international conference* (p. 13).
725 New York, NY, USA: Association for Computing Machinery. Retrieved from
726 <https://doi.org/10.1145/1785455.1785468>